NANO LETTERS

Letter

pubs.acs.org/NanoLett

Active Conformation Control of Unfolded Proteins by Hyperthermal Collision with a Metal Surface

Gordon Rinke,*[,†] Stephan Rauschenbach,*[,†] Ludger Harnau,[‡,§] Alyazan Albarghash,[†] Matthias Pauly,[†,⊥] and Klaus Kern[†,∥]

[†]Max-Planck-Institute for Solid State Research, 70569 Stuttgart, Germany

[‡]IV. Institute for Theoretical Physics, University of Stuttgart, 70174 Stuttgart, Germany

[§]Max-Planck-Institute for Intelligent Systems, 70569 Stuttgart, Germany

[∥]Institut de Physique de la Matière Condensée, École Polytechnique Fédérale de Lausanne, 1015 Lausanne, Switzerland

Supporting Information

ABSTRACT: The physical and chemical properties of macromolecules like proteins are strongly dependent on their conformation. The degrees of freedom of their chemical bonds generate a huge conformational space, of which, however, only a small fraction is accessible in thermal equilibrium. Here we show that soft-landing electrospray ion beam deposition (ES-IBD) of unfolded proteins allows to control their conformation. The dynamics and result of the deposition process can be actively steered by selecting the molecular ion beam's charge state or tuning the incident energy. Using these parameters, protein conformations ranging from fully extended to completely compact can be prepared selectively on a surface, as evidenced on the subnanometer/amino acid resolution level by scanning tunneling microscopy (STM). Supported by molecular dynamics (MD) simulations, our results demonstrate that the final conformation on the surface is reached through a mechanical deformation during the hyperthermal ion surface collision. Our experimental results independently confirm the findings of ion mobility spectrometry (IMS) studies of protein gas phase conformations. Moreover, we establish a new route for the processing of macromolecular materials, with the potential to reach conformations that would be inaccessible otherwise.

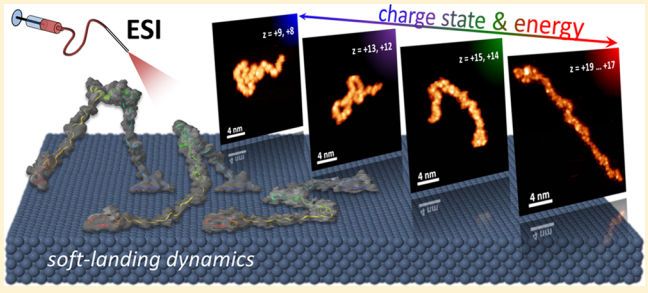

KEYWORDS: *Protein, surface, soft landing, ion beam deposition, scanning tunneling microscopy, charge state, persistence length*

The combined degrees of freedom of the many covalent and noncovalent bonds that make up a macromolecule lead to a vast manifold of possible conformations. Which of those structures is adopted often decides about the macromolecule's properties and functionality. Prime examples for this influence of conformation on the properties are biological molecules like proteins, as they are only functional when folded into a native conformation.[1]

One of the most successful and well-established methods to identify proteins and characterize their chemical composition is electrospray ionization mass spectrometry (ESI-MS).[2−6] Although mass spectrometric measurements of proteins are possible with great precision, they do only reveal structural information in combination with other structure-sensitive methods. Fragmentation for instance gives access to the primary structure of the protein. With ion mobility spectrometry (IMS) the collision cross section of molecular ions can be measured, a quantity that is, for instance, connected to secondary or ternary structures of proteins. With this approach it was demonstrated that a conformation very close to the native state of proteins can be preserved upon transfer from solution into the gas phase.[7−11] In this context the charge state of a gas phase protein ion was identified as a key parameter defining the conformation under the influence of repulsive Coulomb forces acting across the protein.[7,8,12] However, the measurement of the collision cross section, which is only one number, does not provide enough information to obtain the atomic details of the molecular conformation. With support of simulations the shape of the protein ion can be approximated, which however does not reflect the entire structural complexity of the protein.

Preparative mass spectrometry makes use of well-defined macromolecular ion beams including retention of the native conformation, which was demonstrated in several instances for proteins and peptides by probing the conformation after deposition.[13−15] Moreover, methods like electrospray ion beam deposition (ES-IBD) are intended to serve in analytical capacity, and also as a means to fabricate materials and functionalize surfaces by leveraging the ability to control charged beams.[16−20] In particular its use in combination with

Received: June 6, 2014
Revised: August 14, 2014
Published: August 27, 2014

dx.doi.org/10.1021/nl502122j | *Nano Lett.* 2014, 14, 5609−5615

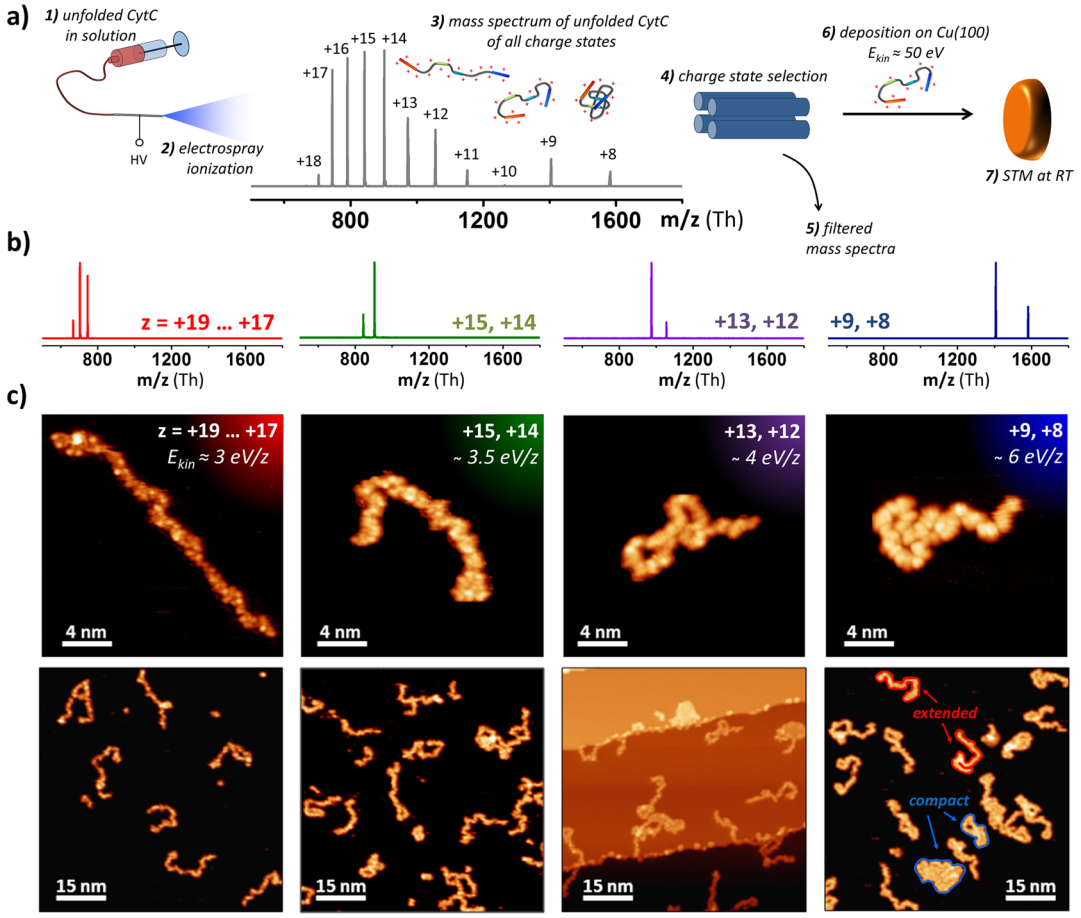

Figure 1. (a) Schematic of the experimental procedure. ESI is used to create gas phase ions of several charge states ranging from z = +8 to z = +19 from a solution of unfolded CytC. After charge state selection, defined species were deposited onto a Cu(100) surface at a constant landing energy of 50 eV and imaged by in situ STM. (b) Mass spectra of the charge state selected CytC ion beams. (c) STM images after deposition of charge state filtered CytC ions on the Cu(100) surface. The protein conformation varies from extended strands for highly charged proteins to compact folded two-dimensional patches for proteins of low charge state.

highly resolving, surface-sensitive methods like scanning tunneling microscopy (STM) offers the advantage of revealing more detailed information about structurally complex objects such as proteins and their interaction with each other and the surface.[15] While the analytical use and nanostructure/thin film growth capacity of molecular ion beam deposition is well established, little is known about the dynamics of the landing process and the effect of the hyperthermal kinetic energy collisions on the conformation of the macromolecular ions.

In this study we demonstrate the capability of defining the conformation of unfolded proteins by their controlled hyperthermal deposition on metal surfaces in vacuum with ES-IBD. Both, choosing the kinetic energy and selecting the charge state, independently enable us to influence the interaction with the surface as well as the gas phase conformation of the ions to be deposited directly. We characterize the deposited proteins with spatial resolution at the amino acid level using in situ STM and employ quantitative image analysis. Surface diffusion is excluded even at room temperature by using a strongly interacting Cu(100) substrate. By adjusting the deposition parameters kinetic energy and charge state, we show that it is possible to generate protein conformations ranging from fully extended, almost straight, strands to compact, two-dimensional (2d) refolded patches.

We reason that the interplay of molecular stiffness induced by the charge state and compression applied by the energetic collision forges the observed two-dimensional objects from the original gas phase conformation. These findings are supported by molecular dynamics (MD) simulations covering the whole landing process from the gas phase to the surface. Controlling the conformational degrees of freedom in a hyperthermic surface interaction represents an entirely new pathway to functional molecular nanostructures.

In this study we use cytochrome c (CytC), a protein consisting of 104 amino acids (m = 12384 Da, $C_{524}H_{852}N_{144}O_{151}S_4$), which is a well established system since it was the object of many ESI-MS, IMS, and H/D-exchange studies.[7,8,21−24] In its natural environment, it is of central importance for several processes in electron transfer and apoptosis.[25,26] Ion beams—almost entirely consisting of unfolded CytC—were prepared by ESI under denaturing conditions, i.e., dissolved in a water/methanol mixture made acidic by the addition of 1% formic acid.[27] The mass spectra in Figure 1a show a distribution of peaks located in the range of m/z = 700−1600 Th (Th = u/e, Thomson, the unit of m/z ratio[28]), each peak corresponding to a charge state of the intact protein from z = +8 to z = +19. The observation of these high charge states confirms that the protein ions are largely unfolded. For comparison, native CytC would result in a

dx.doi.org/10.1021/nl502122j | Nano Lett. 2014, 14, 5609−5615

mass spectrum showing charge states from z = +3 to +8 containing mostly globular folded proteins.[27,29,30]

Out of the many charge states in the prepared, largely unfolded protein ion beam, only a few were selected by tuning the transmission of a quadrupole ion guide to a narrow m/z window. We used windows of a width of 100−250 Th, in order to select the charge states z = +19 to +17, z = +15,+14, z = +13, +12, and z = +9,+8, which was verified by mass spectrometry (Figure 1b). Following beam-energy measurements, the ion beams were steered towards a clean Cu(100) surface located in ultrahigh vacuum (UHV). In order to ensure identical soft-landing conditions, the collision energy of the ions was set through a sample bias to 50 eV.[31] After depositing a submonolayer coverage of approximately 15 pAh (pico Ampere hour) on a 4 mm diameter surface area, the sample was transferred to the STM in situ and imaged at room temperature.

Results and Discussion. Independent of the selected charge state, unfolded, immobilized protein strands of random conformation were found lying flat on the surface (Figure 1c). The deposited proteins exhibit a height of 0.2−0.3 nm and a contour length of 26 ± 1 nm. This contour length fits to unfolded proteins resolved at 1 nm length scale presenting a length of 26.4 nm, for instance, due to partially intact α-helices.[15,32,33]

The conformation of the adsorbed proteins depends strongly on the chosen charge state. With decreasing charge state, the protein conformation evolves from extended, almost straight strands (z = 17−19) through more curved strands (z = 14,15 and z = 12,13) to compact patches, in which the polypeptide strand is packed densely in a compact, two-dimensional patch (z = 12,13 and z = 8,9). In addition to the compact structures, more extended protein strands are observed in the images for low charge states (examples are indicated in Figure 1c).

To quantify the influence of the charge state on the conformation, a statistical analysis of the protein contours was performed by applying the worm-like-chain (WLC) model for noninteracting semiflexible polymers.[34] In this model, the contour of a polymer is related to its molecular stiffness in terms of the persistence length l_p. This quantity can be interpreted as the length over which the polymer is approximately straight.

The persistence length l_p can be extracted from the moments of measured end-to-monomer distance curves $R_2(s)$ and $R_4(s)$.[15,34,35] In Figure 2a the ensemble-averaged moment $R_2(s)$ from many proteins is plotted as a function of contour coordinate s for each of the four different charge states together with theoretical curves from the WLC model. Evidently, the slope of the curves decreases with the protein's charge state. We find a persistence length of l_p = 6.3 ± 0.3 nm for the high charge states (z = 17−19) decreasing to l_p = 2.8 ± 0.4 nm for the low charge states (z = 8,9), which is displayed in Figure 2b as a function of the average ion beam charge state z_{avg}.

The molecular stiffness of charged chain-like molecules can be divided into an electrostatic contribution from the charging and an intrinsic stiffness,[36] which are represented by a term proportional to the square of the charge state and a constant offset, respectively. Fitting this persistence length−charge state relationship yields l_p = 1.6 nm + 0.015 nm z_{avg}^2 (gray line in Figure 2b), where the second term reflects the linear superposition of Coulomb pair potentials.[36] While a linear dependence would also fit the data similarly well, only the extrapolation of our data with the z^2 relation predicts a

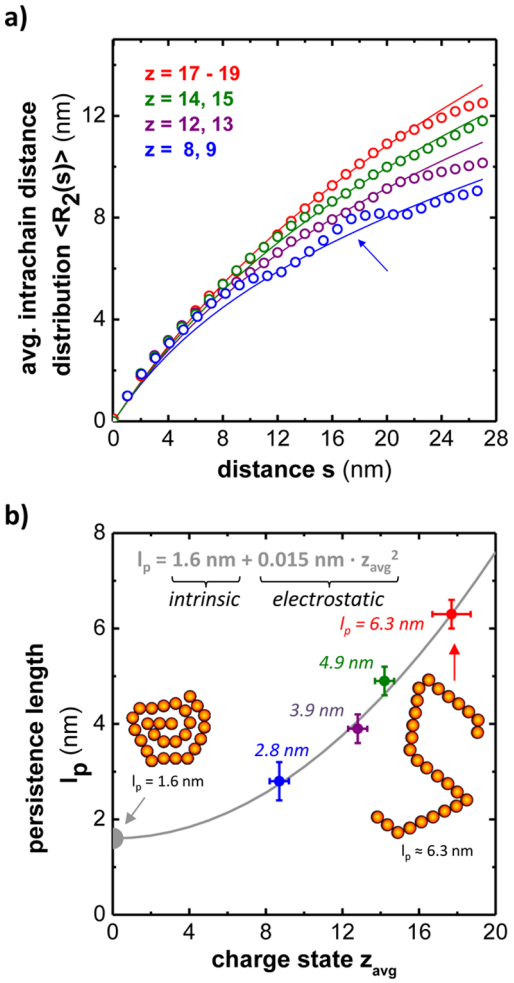

Figure 2. Statistical analysis of the protein conformation from STM images using the WLC model. (a) Measured second moment of the ensemble-averaged end-to-monomer distance $R_2(s)$ from proteins for different charge states (circles) together with theoretical predictions for a free noninteracting polymer (solid lines). (b) Persistence length l_p obtained from the $R_2(s)$ fits for different charge states (symbols). The gray solid line represents a fit of the l_p values as a quadratic function of the average charge state z_{avg}.

persistence length of l_p = 1.6 nm for the uncharged protein, which is consistent with the intrinsic stiffness characterized by the bending rigidity and steric boundary conditions. This value corresponds to a maximal compact, 2d-patch conformation on the surface with an area of approximately 40 nm^2, the area of an individual, compactly backfolded CytC protein, like those measured on a Au(111) surface where the protein ions were neutralized and a most compact 2d-conformation was reached by diffusion.[15] In contrast, the Cu(100) surface interacts strongly with the protein chains, and molecular diffusion is inhibited at room temperature. Consequently, the observed structures must have formed in the gas phase or during the landing process.

More subtle than the charge state dependence of the persistence length are the deviations from the theoretical expectations for a free, noninteracting polymer of the measured $R_2(s)$ and $R_4(s)$ curves. Those deviations indicate that the polymer is interacting with itself and are most pronounced for low charge states (arrow in Figure 2a). Because thermal diffusion does not play a role for the structure formation on the

dx.doi.org/10.1021/nl502122j | Nano Lett. 2014, 14, 5609−5615

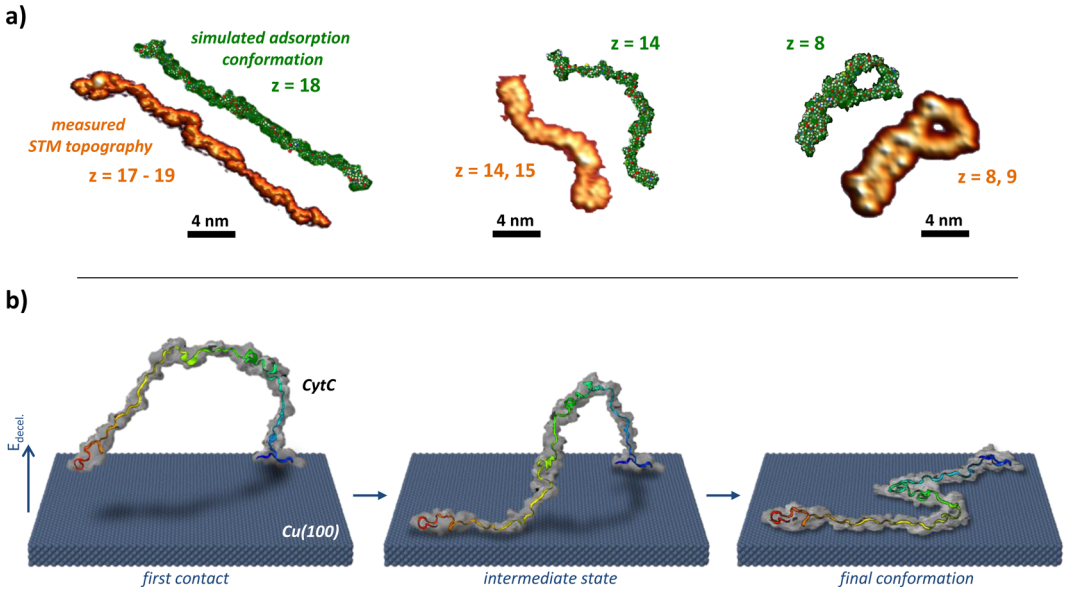

Figure 3. Molecular dynamics simulation of the landing process. (a) Simulated adsorption conformations of unfolded CytC of charge state z = 18, 14, and 8 in comparison with measured STM topographies for charge states z = 17−19, z = 14,15, and z = 8,9. (b) MD simulation of the landing process of a single protein of charge state z = 18. Because of the perpendicular alignment to the surface caused by the dipole moment and the external field, the compressed protein touches the surface first with one end. It is then strongly deformed before the other end touches the surface, while the middle portion is still lifted. Thus, an upright standing arc is formed, which finally adsorbs between the two ends while being further deformed (see also Supporting Information for a video).

Cu(100) surface, the interaction of the peptide strand with itself must be the result of transient mobility directly after the landing process due to the hyperthermal interaction.

To understand the development of the protein conformation on the surface during collision, we investigated the adsorption of CytC ions on a Cu(100) surface in detail by means of MD simulations using the GROMACS software.[37] We considered a fixed charge distribution because the precise location of the charges on CytC after ESI is not known,[24,38−40] and it is not possible to perform computer simulation studies for all the charging site permutations[38] (see Supporting Information for details). As a starting point, protein ions of various charge states were relaxed in vacuum resulting in different initial gas phase structures. Subsequently, we added a velocity and an electric field perpendicular to the sample surface to match the experimental conditions. Upon landing, the protein relaxes into a stable configuration.

Examples for final conformations of CytC on the Cu(100) surface from the simulations of different charge states, are shown in Figure 3a. They exhibit characteristic features similar to actual measured STM topographies shown next to them and recreate the trend from extended to compact conformation upon decreasing the charge state. Especially in the case of low charge state CytC (z = 8), the characteristic tight loops with 180° back-fold are reproduced by the MD simulations. Here, lowly charged sections along the backbone act like flexible hinges that allow for an interaction of the protein strand with itself, leading to the characteristic compact patches observed in STM. We emphasize that the three simulated protein conformations shown in Figure 3a have to be considered as representatives of three statistical ensembles implying that various additional conformations can be found in MD simulations. However, the conformations shown in Figure 3a exhibit characteristic features of the charge state. For example, we have not found a fully stretched protein for the charge state z = 8 or tight loops with 180° back-folds for the charge state z = 18.

The dynamics of the deposition process is illustrated in Figure 3b in three snap shots over a time of 180 ps of a CytC landing simulation for z = 18 (see Supporting Information for an animation). Apart from the deceleration, the effect of the electric field is in interaction with the relatively large electric dipole moment of the protein ion; for instance, 330 Dy for native CytC caused by inhomogeneous charge distributions.[41] This provokes a partial alignment of the protein strand such that they touch the surface first with atoms located close to one of their ends. Because of its stiffness, it then buckles until the other end touches the surface and binds to it. The middle portion remains elevated, forming an upright standing arc, which finally adsorbs between the two ends, while deforming itself into the final s-shaped conformation.

The landing sequence (Figure 3b) readily shows how the different conformations arise as a consequence of the Coulomb interaction. The charge state of the protein ion directly defines the molecular stiffness as well as the three-dimensional gas phase conformation.[8] During the ion−surface collision, the extended, three-dimensional, initial gas phase conformation is reduced into a two-dimensional adsorption geometry. Conditioned by the charge state induced molecular stiffness, the characteristic bending radii of the proteins form as a response to the strain induced by the interaction with the surface. Hence, extended or compact conformations are observed on the surface for higher or lower charge states, respectively. Because of the central role of the initial gas phase conformation, the observed dependence of conformation on the charge state independently confirms the findings from ion mobility spectrometry for the gas phase conformation of proteins.

Deviations from the discussed, near perpendicular alignment of protein strand and surface are likely because the gas phase conformations are complex three-dimensional shapes that may exhibit additional rotational and vibrational motion, originating

dx.doi.org/10.1021/nl502122j | Nano Lett. 2014, 14, 5609−5615

from passing through the ion optics. Indeed an oscillatory motion of the protein dipole axis with respect to the electric field would lead to a distribution of orientations around the most probable angle of incidence. Therefore, we also consider the case of a preferably parallel alignment of proteins in the gas phase and surface, in which little deformation would occur and the conformation would just be a projection of the 3d gas phase conformation onto the surface (see Supporting Information). For a distribution of protein conformations this implies that some, more perpendicular oriented ions undergo significant deformation while other, predominantly parallel oriented ions remain mostly unperturbed. This offers an explanation for the spread of conformations observed especially for low charge states, where we find compact patches alongside with extended strands as indicated in Figure 1c. The coexistence of these very different conformations confirms that for soft proteins the orientation with respect to the surface at the onset of the landing causes the difference between a compact refolded patch for a perpendicular landing orientation and a curved, yet extended strand for a parallel landing orientation. Highly charged, stiff proteins, however, are less likely to change their gas phase conformation upon collision that strongly.

The landing simulations as well as the deposition results indicate that the proteins are deformed upon landing. Starting from a gas phase conformation, this deformation occurs as a consequence of the release of kinetic energy during the collision, which is acting against the stiffness of the charged protein, defined by the charge state. This model of the landing process predicts that the protein conformation can be influenced by the landing energy, a parameter that can be readily adjusted in ES-IBD simply by applying a sample bias voltage. By increasing the kinetic energy of the ions, the influence of the repulsive Coulomb forces can be compensated during the collision leading to enhanced buckling and more compact final protein conformations. To pursue this strategy, we performed additional experiments in which the landing energy was increased to several hundred electron volts. The samples were characterized after deposition by STM as before, including the quantitative analysis following the WLC model.

A reduction of the persistence length with kinetic energy was observed for high charge state protein ions. Decreasing from an initial value of 6.3 ± 0.4 nm for 50 eV, the persistence length levels out at 4.5 ± 0.3 nm for landing energies above 150 eV (red symbols in Figure 4). For low charge state proteins the persistence length remains approximately constant at 2.6 ± 0.4 nm as measured at 50 and 250 eV (blue symbols in Figure 4). Indeed considering the distribution of extended and very compact shapes at low energy, a further reduction of the persistence length for low charge state ions is not to be expected. Upon increasing the energy to 1000 eV, only small fragments of the protein of sizes not longer than 10 nm were found on the surface showing the transition to surface induced dissociation (see Supporting Information).[42]

A comparison of the energy scales rationalizes this observation. Between the highest and lowest charge states used in our experiments $z = 18$ and $z = 8$ lies an order of magnitude of Coulomb energy (20.3 and 2.5 eV, respectively).[8,38,43] In the initial experiment a kinetic energy of 50 eV was used for all charge states. A fraction of this energy (typically 5−35%)[42] remains in the ion as internal energy upon collision, while the rest dissipates in the substrate or is converted in other processes.[42,44−47] Compared to the Coulomb energy for $z = 8$, the kinetic energy is much larger, whereas it is of the same order in magnitude as the Coulomb energy for $z = 18$. Hence, highly charged molecules not only exhibit an extended gas phase conformation but the charge-induced rigidity also causes the conformation to be preserved upon an energetic collision with the surface. Lowly charged molecular species, however, are more compact and also easier to be deformed.

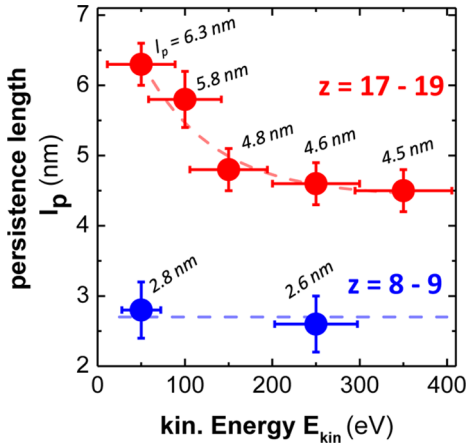

Figure 4. Persistence length l_p of high and low charge state proteins as a function of the landing energy. Low charge state proteins exhibit a constant l_p (blue), whereas the persistence length for the high charge state proteins decreases with landing energy (red). The dashed lines indicate their trends.

To this point, we have considered a fixed charge distribution on a protein during the whole adsorption process. However, in principle the possibility of neutralization of the protein ions upon contact with the copper surface has to be taken into account. To investigate a potential link between discharging of adsorbed proteins and their final conformation, we have performed additional simulations of adsorbing uncharged CytC using the MD results shown in Figure 3a as initial systems. These simulations resulted in very similar final protein conformations, with minor variations of the location of some amino acids. We conclude that, within the limits of the present MD simulations, no major conformational changes of the adsorbed proteins upon discharging occur. This result applies specifically to the case of a Cu(100) surface due to the strong van der Waals interactions between proteins and this surface as compared to intramolecular protein interactions. Preliminary simulations of CytC adsorption on surfaces with weaker protein−surface van der Waals interactions exhibit a two-dimensionally confined refolding upon discharging after adsorption.[15] We note that these conclusions rest on classical MD simulations, which do not allow one to study proton transfer.

Conclusions. The observed energy dependence supports the view of a landing process in which the final surface conformation of the protein is reached as the result of the interplay of molecular stiffness induced by Coulomb repulsion and deformation controlled by the landing energy. This model is in agreement with all other observations, like the conformation distribution imaged in STM and the dynamics observed by MD simulations.

By using ES-IBD, we have demonstrated a method that allows us to control the conformation of individual, unfolded proteins or, more generally polymers, through parameters that can be actively set, simply by adjusting voltages applied to the ion optics of the deposition source. In addition to the chemical

dx.doi.org/10.1021/nl502122j | Nano Lett. 2014, 14, 5609−5615

purity that is provided by mass selection and mass spectrometry, as well as the quantitative control over the coverage by measuring the ion current, we show that ES-IBD is a unique tool offering unprecedented control over many deposition parameters, greatly extending the possibility over conventional methods like thermal evaporation, which anyhow is not capable to handle large, nonvolatile molecules.

As a result, it is possible to manufacture coatings of selected protein conformation, to study their properties, or use the high resolution of scanning probe microscopes to gain additional information about the conformation of a given gas phase object. The latter is particularly interesting for biological objects like viruses, antibodies, or glycanes.[48] For instance, the fully extended strand shown in Figure 1 enables access to each amino acid individually by a scanning probe microscope. Understanding the role of certain amino acids and their interaction at the atomic level with respect to the conformation and functionality on the surface would enable mimicking nature's design of functional nanostructures by folding in two dimensions.

It is moreover clear that the methodology of depositing ion beams as a coating technique has great potential to be extended in further studies. Controlling the ion motion with greater precision in space and energy, as already shown for single atomic ions,[49] could allow additional control over the dynamics of the collision with the surface and adjust the conformation more precisely or even induce chemical interactions.

Methods. Solutions of cytochrome c (CytC) (Sigma-Aldrich, C2506) for mass spectrometry and subsequent deposition experiments were prepared by dissolving CytC in water/methanol mixtures. With the addition of 1% formic acid to the solution, it was ensured that the proteins were unfolded.[27] Positively charged gas phase ions were created with a nanospray emitter at 3−4 kV and a flow rate of 15 μL/h. After transfer into vacuum, the ions were mass-selected with a radio frequency-quadrupole in a way that only ions characterized by a certain narrow mass-to-charge (m/z) ratio pass. Subsequently, time-of-flight mass spectrometry (TOF-MS) and energy detection at a pressure of 10^{-8} mbar ensured a defined ion beam.

For the deposition on a Cu(100) sample, which was cleaned with several sputter and annealing cycles, the ion beam was further guided through two following apertures leading to the deposition chamber at a pressure of 10^{-10} mbar. A positive voltage V_s applied to the sample decelerated the ions for soft landing to the collision energy of $E_{coll} = E_{kin} + V_s z$.[50] The ion current of the sample was monitored online using electrometers (Keithley 616). After deposition, the sample was transferred in situ to a variable temperature STM (Omicron VT-STM, Omicron Nanotechnology GmbH, Germany) and was scanned at room temperature (RT).

For the analysis with the WLC model, several samples and STM images were evaluated and the conformation of 50−100 individual, clearly identified molecules with a length of 25 ± 4 nm are considered for each charge state measurement. Proteins that are adsorbed mainly at step edges are excluded from the analysis. These rules were applied to all data sets identically so that the obtained results are comparable to each other.

■ ASSOCIATED CONTENT

Supporting Information

Detailed description of the experiment, details of the data analysis, details about the MD simulation with additional data, considerations about the Coulomb energy, and data on the fragmentation on the surface. This material is available free of charge via the Internet at http://pubs.acs.org.

■ AUTHOR INFORMATION

Corresponding Authors

*(G.R.) E-mail: g.rinke@fkf.mpg.de.
*(S.R.) E-mail: s.rauschenbach@fkf.mpg.de.

Present Address

⊥(M.P.) Institut Charles Sadron, CNRS-University of Strasbourg, Strasbourg, France.

Notes

The authors declare no competing financial interest.

■ ACKNOWLEDGMENTS

The authors would like to thank Dr. Rico Gutzler, Dr. Girjesh Dubey, and Prof. Dr. Frank Sobott for fruitful discussions.

■ REFERENCES

(1) Petsko, G. A.; Ringe, D. *Protein Structure and Function*; New Science Press, Ltd.: London, U.K., 2004.
(2) Yates, J. R. *J. Mass Spectrom.* **1998**, *33*, 1−19.
(3) Rout, M. P.; Aitchison, J. D.; Suprapto, A.; Hjertaas, K.; Zhao, Y. M.; Chait, B. T. *J. Cell Biol.* **2000**, *148*, 635−651.
(4) Benesch, J. L. P.; Ruotolo, B. T.; Simmons, D. A.; Robinson, C. V. *Chem. Rev.* **2007**, *107*, 3544−3567.
(5) Barrera, N. P.; Di Bartolo, N.; Booth, P. J.; Robinson, C. V. *Science* **2008**, *321*, 243.
(6) Breuker, K.; Brüschweiler, S.; Tollinger, M. *Angew. Chem., Int. Ed.* **2010**, *50*, 873−877.
(7) Clemmer, D. E.; Hudgins, R. R.; Jarrold, M. F. *J. Am. Chem. Soc.* **1995**, *117*, 10141−10142.
(8) Shelimov, K. B.; Clemmer, D. E.; Hudgins, R. R.; Jarrold, M. F. *J. Am. Chem. Soc.* **1997**, *119*, 2240−2248.
(9) Warnke, S.; von Helden, G.; Pagel, K. *J. Am. Chem. Soc.* **2013**, *135*, 1177−1180.
(10) Hall, Z.; Robinson, C. V. *J. Am. Soc. Mass Spectrom.* **2012**, *23*, 1161−1168.
(11) Brady, J. J.; Judge, E. J.; Levis, R. J. *Proc. Natl. Acad. Sci. U.S.A.* **2011**, *108*, 12217−12222.
(12) Kaltashov, I. A.; Eyles, S. J. *Mass Spectrom. Rev.* **2002**, *21*, 37−71.
(13) Ouyang, Z.; Takats, Z.; Blake, T. A.; Gologan, B.; Guymon, A. J.; Wiseman, J. M.; Oliver, J. C.; Davisson, V. J.; Cooks, R. G. *Science* **2003**, *301*, 1351−1354.
(14) Wang, P.; Laskin, J. *Angew. Chem., Int. Ed.* **2008**, *47*, 6678−668.
(15) Deng, Z.; Thontasen, N.; Malinowski, N.; Rinke, G.; Harnau, L.; Rauschenbach, S.; Kern, K. *Nano Lett.* **2012**, *12*, 2452−2458.
(16) Franchetti, V.; Solka, B. H.; Baitinger, W. E.; Amy, J. W.; Cooks, R. G. *Int. J. Mass Spectrom. Ion Processes* **1977**, *23*, 29−35.
(17) Miller, S. A.; Luo, H.; Pachuta, S. J.; Cooks, R. G. *Science* **1997**, *275*, 1447−1450.
(18) Laskin, J.; Wang, P.; Hadjar, O. *Phys. Chem. Chem. Phys.* **2008**, *10*, 1079−1090.
(19) Rauschenbach, S.; Stadler, F. L.; Lunedei, E.; Malinowski, N.; Koltsov, S.; Costantini, G.; Kern, K. *Small* **2006**, *2*, 540−547.
(20) Rauschenbach, S.; Rinke, G.; Malinowski, N.; Weitz, R. T.; Dinnebier, R.; Thontasen, N.; Deng, Z.; Lutz, T.; de Almeida Rollo, P. M.; Costantini, G.; Harnau, L.; Kern, K. *Adv. Mater.* **2012**, *24*, 2761−2767.
(21) Fenn, J. B.; Mann, M.; Meng, C. K.; Wong, S. F.; Whitehouse, C. M. *Mass Spectrom. Rev.* **1990**, *9* (37−70), 76.
(22) Wood, T. D.; Chorush, R. A.; Wampler, F. M.; Little, D. P.; O'Connor, P. B.; McLafferty, F. W. *Proc. Natl. Acad. Sci. U. S. A.* **1995**, *92*, 2451−2454.
(23) Hoaglund-Hyzer, C. S.; Counterman, A. E.; Clemmer, D. E. *Chem. Rev.* **1999**, *99* (3037−3079), 341.

(24) Breuker, K. *Int. J. Mass Spectrom.* **2006**, *253*, 249.
(25) Jain, R. K.; Hamilton, A. D. *Org. Lett.* **2000**, *2*, 1721−1723.
(26) Moore, G. R.; Pettigrew, G. W. *Cytochromes C: Evolutionary, Structural And Physicochemical Aspects*; Springer-Verlag: Berlin, Germany, 1990.
(27) Konermann, L.; Douglas, D. J. *Biochemistry* **1997**, *36* (12296−12302), 51.
(28) Cooks, R. G.; Rockwood, A. L. *Rapid Commun. Mass Spectrom.* **1991**, *5*, 93.
(29) Clemmer, D.; Jarrold, M. F. *J. Mass Spectrom.* **1997**, *32*, 577−592.
(30) Cassou, C. A.; Sterling, H. J.; Susa, A. C.; Williams, E. R. *Anal. Chem.* **2013**, *85*, 138−146.
(31) Rauschenbach, S.; Vogelgesang, R.; Malinowski, N.; Gerlach, J. W.; Benyoucef, M.; Costantini, G.; Deng, Z.; Thontasen, N.; Kern, K. *ACS Nano* **2009**, *3*, 2901.
(32) Wolynes, P. G. *Proc. Natl. Acad. Sci. U.S.A.* **1995**, *92*, 2426−2427.
(33) Tkatchenko, A.; Rossi, M.; Blum, V.; Ireta, J.; Scheffler, M. *Phys. Rev. Lett.* **2011**, *106*, 118102.
(34) Harnau, L.; Winkler, R. G.; Reineker, P. *J. Chem. Phys.* **1996**, *104*, 6355.
(35) Doi, M.; Edwards, S. F. *The Theory of Polymer Dynamics*; Oxford University Press: Oxford, U.K., 1986.
(36) Toan, N. M.; Ha, B.-Y.; Thirumalai, D. Polyelectrolyte and Polyampholyte Effects in Synthetic and Biological Macromolecules. In *Ionic Interactions in Natural and Synthetic Macromolecules*; Ciferri, A., Perico, A., Eds.; John Wiley and Sons:Hoboken, NJ, 2012.
(37) van der Spoel, D.; Marklund, E. G.; Larsson, D. S. D.; Caleman, C. *Macromol. Biosci.* **2011**, *11*, 50−59.
(38) Schnier, P. D.; Gross, D. S.; Williams, E. R. *J. Am. Chem. Soc.* **1995**, *110*, 6747−6757.
(39) Mao, Y.; Woenckhaus, J.; Kolafa, J.; Ratner, M. A.; Jarrold, M. F. *J. Am. Chem. Soc.* **1999**, *121*, 2712−2721.
(40) Steinberg, M. Z.; Elber, R.; McLafferty, F. W.; Gerber, R. B.; Breuker, K. *ChemBioChem* **2008**, *13*, 2417.
(41) Koppenol, W. H.; Rush, J. D.; Mills, J. D.; Margolias, E. *Mol. Biol. Evol.* **1991**, *8*, 545−558.
(42) Cyriac, J.; Pradeep, T.; Kang, H.; Souda, R.; Cooks, R. G. *Chem. Rev.* **2012**, *112*, 5356−5411.
(43) Rockwood, A. L.; Busman, M.; Smith, R. D. *Int. J. Mass Spectrom. Ion Proc.* **1991**, *111*, 103−129.
(44) Bromann, K.; Felix, C.; Brune, H.; Harbich, W.; Monot, R.; Buttet, J.; Kern, K. *Science* **1996**, *274* (956−958), 26.
(45) Cheng, H. P.; Landman, U. *Science* **1993**, *260* (1304−1307), 38.
(46) Grill, V.; Shen, J.; Evans, C.; Cooks, R. G. *Rev. Sci. Instrum.* **2001**, *72*, 3149−3179.
(47) Gologan, B.; Green, J. R.; Alvarez, J.; Laskin, J.; Cooks, R. G. *Phys. Chem. Chem. Phys.* **2005**, *7*, 1490−1500.
(48) Snijder, J.; Rose, R. J.; Veesler, D.; Johnson, J. E.; Heck, A. J. R. *Angew. Chem., Int. Ed.* **2013**, *52*, 4020−4023.
(49) Schnitzler, W.; Linke, N. M.; Fickler, R.; Meijer, J.; Schmidt-Kaler, F.; Singer, K. *Phys. Rev. Lett.* **2009**, *102*, 070501.
(50) Mikhailov, V. A.; Mize, T. H.; Benesch, J. L.; Robinson, C. V. *Anal. Chem.* **2014**, *86*, 8321−8328.